Multilayered Media Green's Functions in Integral Equation Formulations

Article *in* IEEE Transactions on Antennas and Propagation · April 1997

DOI: 10.1109/8.558666 · Source: IEEE Xplore

2 authors:

Krzysztof Michalski
Texas A&M University
91 PUBLICATIONS **2,467** CITATIONS
SEE PROFILE

Juan R. Mosig
École Polytechnique Fédérale de Lausanne
552 PUBLICATIONS **4,858** CITATIONS
SEE PROFILE

Multilayered Media Green's Functions in Integral Equation Formulations

Krzysztof A. Michalski, *Senior Member, IEEE*, and Juan R. Mosig, *Senior Member, IEEE*

Invited Review Paper

***Abstract*—A compact representation is given of the electric- and magnetic-type dyadic Green's functions for plane-stratified, multilayered, uniaxial media based on the transmission-line network analog along the axis normal to the stratification. Furthermore, mixed-potential integral equations are derived within the framework of this transmission-line formalism for arbitrarily shaped, conducting or penetrable objects embedded in the multilayered medium. The development emphasizes laterally unbounded environments, but an extension to the case of a medium enclosed by a rectangular shield is also included.**

***Index Terms*— Green's functions, integral equations, layered media.**

I. Introduction

In a variety of applications, such as geophysical prospecting [1]–[3], remote sensing [4], wave propagation [5], [6], and microstrip circuits and antennas [7]–[9], it is necessary to compute the electromagnetic field in a layered medium. For a given set of sources, the field may easily be found if the dyadic Green's functions (DGF's) of the environment are available. Numerous authors have derived DGF's for layered media, both isotropic and anisotropic [10]–[31]. Most of the recent developments in this area have been driven by applications to microstrip patch antennas, printed circuit boards, and monolithic microwave/millimeter-wave integrated circuits.

When the currents are not known *a priori*, which is usually the case in scattering and antenna problems, the DGF's may be used to formulate integral equations for the true or equivalent currents, which are then solved numerically by the method of moments (MOM) [32]. The hypersingular behavior of some of the integral equation kernels causes difficulties in the solution procedure [33], which may be avoided if the fields are expressed in terms of vector and scalar potentials with weakly singular kernels. This led to the development of mixed-potential integral equations (MPIE's) for arbitrarily shaped scatterers in free space [34]–[37]. In layered media, an important advantage of the MPIE's is that the spectral Sommerfeld-type integrals (or series, in the case of laterally shielded environments) appearing in the potential kernels converge more rapidly and are easier to accelerate than those associated with the field forms that are, in effect, obtained by differentiation of the potentials. This was recognized early on by Mosig and Gardiol [38]–[40], who derived and successfully applied an MPIE for planar microstrip structures on a grounded substrate. This MPIE could not easily be extended to general nonplanar conductors, because—as was later realized—in layered media the scalar potential kernels associated with horizontal and vertical current components were different [41], [42]. However, ways to handle vertical probe feeds were soon devised, incorporating both the "horizontal" and "vertical" scalar potential kernels [43]–[46]. Since different kernels were used for the horizontal and vertical currents, a fictitious point charge had to be introduced at the feed point. Other "two-potential" MPIE formulations were also proposed to tackle vertical probes [47], [48]. The development of efficient procedures for the computation of the Sommerfeld integrals [38] and an extension to multilayered media [44] made the MPIE an attractive approach for planar microstrip circuit and antenna problems [49]–[59].

To tackle arbitrarily shaped, three-dimensional (3-D) conducting objects, Michalski [41] proposed to use the "horizontal" scalar potential kernel throughout, which necessitated a proper "correction" of those elements of the dyadic vector potential kernel associated with the vertical current component. This approach was later put on firmer theoretical basis by Michalski and Zheng [60], who described three distinct MPIE formulations (referred to as A, B, and C) for multilayered media and discussed their relative merits. One of these MPIE's (formulation C), which was deemed preferable for objects penetrating an interface, was implemented and validated for the case of a two-layer medium [61]. Furthermore, the MPIE of Mosig and Gardiol and other previously used MPIE's [62]–[64] were classified as special cases of the newly developed formulations. The formulation C MPIE was later applied to microstrip transmission lines of arbitrary cross section [65], vertical probe-fed microstrip patch antennas [66], arbitrarily shaped microstrip patch resonators in uniaxial substrates [67], and printed spiral antennas [68]. Recently, modified MPIE's were proposed, in which the scalar potential (rather than the vector potential kernel) is "corrected" [69]–[71]. Alternative derivations of the three MPIE formulations for multilayered

Manuscript received June 11, 1996; revised October 7, 1996.

K. A. Michalski is with the Department of Electrical Engineering, Electromagnetics and Microwave Laboratory, Texas A&M University, College Station, TX 77843 USA.

J. R. Mosig is with the Laboratory of Electromagnetics and Acoustics, Swiss Federal Institute of Technology, EPFL-Ecublens Lausanne, CH-1015, Switzerland.

Publisher Item Identifier S 0018-926X(97)02299-0.

uniaxial media were also presented [72], [73]. More recently, the formulation C MPIE was adopted to analyze electromagnetic scattering by wires [74] and conducting bodies of revolution [75], [76] buried in earth.

In this paper, we present a compact formulation of the electric- and magnetic-type DGF's for plane-stratified, multilayered uniaxial media, based on the transmission-line network analog along the axis normal to the stratification [77]. Furthermore, we derive within the framework of this transmission-line formalism MPIE's for arbitrarily shaped, penetrable or conducting objects embedded in the multilayered medium. Attention is limited to media with at most uniaxial anisotropy, which while being important in practice [78]–[80], still allow the simple transmission-line representation of the electromagnetic fields. The emphasis is on laterally unbounded environments, but an extension to the case of a layered medium enclosed by a rectangular shield is also included.

The remainder of this paper is organized as follows. In Section II, we outline the formulation of the integral equations for penetrable or perfectly conducting objects embedded in a layered medium. In Section III, we introduce the Fourier transform formalism and express the spectral fields in terms of the voltages and currents on the transmission-line analog of the medium. In Section IV, we formulate the DGF's for a medium with an as yet unspecified stratification in terms of the transmission-line Green's functions (TLGF's). In Section V, we derive MPIE's for arbitrarily shaped, three-dimensional objects embedded in such a medium and express their kernels in terms of the TLGF's. In Section VI, we specialize the formulation for multilayered media with piecewise-constant parameters and give a practical algorithm for the efficient computation of the TLGF's. In Section VII, we briefly discuss the treatment of the Sommerfeld integrals. In Section VIII, we extend the formulation to the practically important case of a medium shielded by a rectangular enclosure. In Section IX, we make some concluding remarks.

The $e^{j\omega t}$ time dependence is implicit in the formulation and the stratification is assumed to be transverse to the z axis of the Cartesian (x, y, z)-coordinate system. Source coordinates are distinguished by primes, vectors are denoted by boldface letters, unit vectors are distinguished by carets, and dyadics are denoted by doubly underlined boldface letters.

II. Formulation of Integral Equations

Consider an arbitrarily shaped object embedded in a layered medium and excited by known electric and magnetic currents $(\boldsymbol{J}^i, \boldsymbol{M}^i)$, as illustrated in Fig. 1(a). The equations governing the resulting electric and magnetic fields $(\boldsymbol{E}, \boldsymbol{H})$ are most easily derived by means of the equivalence principle [81, p. 106]. An *external* equivalent problem is shown in Fig. 1(b), where the surface currents $(\boldsymbol{J}_s, \boldsymbol{M}_s)$ and the *impressed* currents $(\boldsymbol{J}^i, \boldsymbol{M}^i)$ radiating in the layered medium produce the correct fields $(\boldsymbol{E}, \boldsymbol{H})$ exterior to S and null fields inside S. Clearly, $(\boldsymbol{E}, \boldsymbol{H}) = (\boldsymbol{E}^i + \boldsymbol{E}^s, \boldsymbol{H}^i + \boldsymbol{H}^s)$, where $(\boldsymbol{E}^i, \boldsymbol{H}^i)$ are the *impressed* fields due to $(\boldsymbol{J}^i, \boldsymbol{M}^i)$ and $(\boldsymbol{E}^s, \boldsymbol{H}^s)$ are the *scattered* fields due to $(\boldsymbol{J}_s, \boldsymbol{M}_s)$. The boundary conditions at

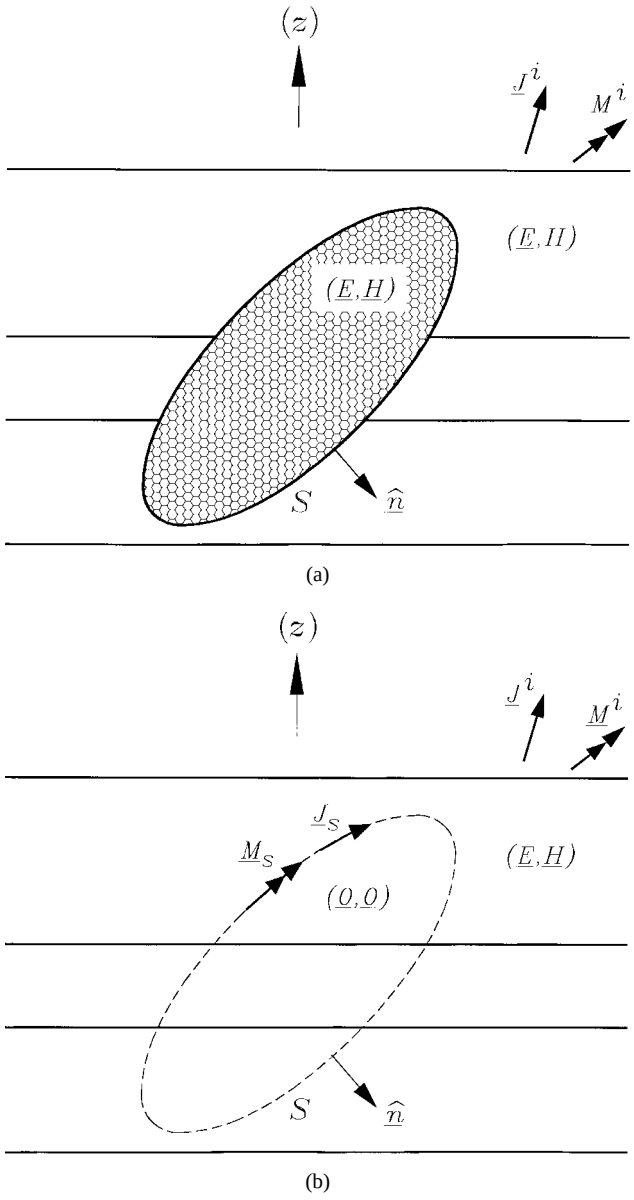

Fig. 1. Arbitrarily shaped object in a layered medium. (a) Physical configuration. (b) External equivalent problem.

S dictate that

$$\boldsymbol{M}_s = -\hat{\boldsymbol{n}} \times (\boldsymbol{E}^i + \boldsymbol{E}^s[\boldsymbol{J}_s, \boldsymbol{M}_s])_{S_+} \tag{1}$$

$$\boldsymbol{J}_s = \hat{\boldsymbol{n}} \times (\boldsymbol{H}^i + \boldsymbol{H}^s[\boldsymbol{J}_s, \boldsymbol{M}_s])_{S_+} \tag{2}$$

where $\hat{\boldsymbol{n}}$ is the outward unit vector normal to S and the subscript S_+ indicates that the fields are evaluated as the observation point approaches S from the exterior region. In linear media, the fields due to arbitrary current distributions $(\boldsymbol{J}, \boldsymbol{M})$ may be expressed as

$$\boldsymbol{E} = \langle \underline{\underline{\boldsymbol{G}}}^{EJ}; \boldsymbol{J} \rangle + \langle \underline{\underline{\boldsymbol{G}}}^{EM}; \boldsymbol{M} \rangle \tag{3}$$

$$\boldsymbol{H} = \langle \underline{\underline{\boldsymbol{G}}}^{HJ}; \boldsymbol{J} \rangle + \langle \underline{\underline{\boldsymbol{G}}}^{HM}; \boldsymbol{M} \rangle \tag{4}$$

where $\underline{\underline{\boldsymbol{G}}}^{PQ}(\boldsymbol{r}|\boldsymbol{r}')$ is the DGF relating P-type fields at $\boldsymbol{r}$ and Q-type currents at $\boldsymbol{r}'$. The notation $\langle\ ,\ \rangle$ is used for integrals of products of two functions separated by the comma over their common spatial support, with a dot over the comma indicating

a dot product. Since the DGF's for the layered medium of Fig. 1(b) are available, one can use (3) and (4) to compute the impressed fields and to express the scattered fields in (1) and (2) in terms of the unknown currents $(\boldsymbol{J}_s, \boldsymbol{M}_s)$.

For penetrable objects, an interior equivalent problem may be constructed, in which the surface currents $(-\boldsymbol{J}_s, -\boldsymbol{M}_s)$, radiating in the presence of the object, produce the correct fields $(\boldsymbol{E}, \boldsymbol{H})$ inside S and null fields outside. If the object is homogeneous, its medium may be extended to fill the entire space and the homogeneous medium DGF's may used in (3) and (4) to compute the fields. A set of two equations similar to (1) and (2) may then be written for the interior problem and combined with those of the exterior problem to yield a coupled set uniquely solvable for $(\boldsymbol{J}_s, \boldsymbol{M}_s)$ [82]. For inhomogeneous objects, DGF's associated with the interior equivalent problem are not available and (1) and (2) must be augmented by the differential equations governing the fields inside the volume enclosed by S. This leads to a set of hybrid integro-differential equations for $(\boldsymbol{J}_s, \boldsymbol{M}_s)$ and the fields inside the objects [83]–[86]. An alternative procedure, applicable to both homogeneous and inhomogeneous objects, is to replace the object in the interior equivalent problem with electric and magnetic volume polarization currents radiating in free space [36], [81, p. 126]. As a result, a set of hybrid volume-surface integral equations is obtained [87]. An advantage of this approach is that—unlike in the standard domain integral equation methods [23], [27]—there are no Sommerfeld integrals associated with the interior problem.

Nonperfect conductors can often be modeled as surface impedance objects characterized by the impedance boundary condition (IBC) $\boldsymbol{M}_s = Z_s \boldsymbol{J}_s \times \hat{\boldsymbol{n}}$, where Z_s is the skin effect surface impedance [88], [89]. One can use this IBC in either (1) or (2) to eliminate $\boldsymbol{M}_s$. The resulting equations are referred to, respectively, as the electric-field integral equation (EFIE) and the magnetic-field integral equation (MFIE). Only the EFIE is applicable to open, infinitesimally thick shells made of a perfect electric conductor (PEC). In the analysis of microstrip structures, it is common to use a simplified form of the EFIE, which neglects the contribution of $\boldsymbol{M}_s$ to $\boldsymbol{E}^s$ [90]. For closed-impedance or PEC objects, either the EFIE or the MFIE or their combination known as the combined-field integral equation (CFIE), may be used to solve for $\boldsymbol{J}_s$. The CFIE does not suffer from the internal resonance problems that plague the EFIE and the MFIE [91].

There are important applications where the object in Fig. 1(a) is excited through an aperture in a PEC plane. In such cases the aperture is "shorted" and an equivalent magnetic surface current is placed over the shorted region to support the correct electric field there. The contribution of this current is then included in (1) and (2). Since the equivalent aperture current is typically unknown, the MPIE's are supplemented by an integral equation obtained by enforcing the continuity of the tangential magnetic field across the aperture [92].

In view of the hypersingular behavior of $\underline{\underline{\boldsymbol{G}}}^{EJ}$ and $\underline{\underline{\boldsymbol{G}}}^{HM}$, it is preferable to convert (3) and (4) into their mixed-potential forms before they are used in (1) and (2). In this process, one encounters the previously mentioned dilemma caused by the fact that in layered media the scalar potential kernels associated with the horizontal and vertical current components are in general different [42]. Consequently, either the scalar or the vector potential kernel must be modified for arbitrary current distributions. We show in Section V that choosing the former route [69], [70] leads to the mixed-potential forms

$$\boldsymbol{E} = -j\omega\mu_0 \langle \underline{\underline{\boldsymbol{G}}}^A; \boldsymbol{J} \rangle + \frac{1}{j\omega\varepsilon_0} \nabla (\langle K^\Phi, \nabla' \cdot \boldsymbol{J} \rangle + \langle C^\Phi \hat{\boldsymbol{z}}; \boldsymbol{J} \rangle) + \langle \underline{\underline{\boldsymbol{G}}}^{EM}; \boldsymbol{M} \rangle \tag{5}$$

$$\boldsymbol{H} = \langle \underline{\underline{\boldsymbol{G}}}^{HJ}; \boldsymbol{J} \rangle - j\omega\varepsilon_0 \langle \underline{\underline{\boldsymbol{G}}}^F; \boldsymbol{M} \rangle + \frac{1}{j\omega\mu_0} \nabla (\langle K^\Phi, \nabla' \cdot \boldsymbol{M} \rangle + \langle C^\Psi \hat{\boldsymbol{z}}; \boldsymbol{M} \rangle) \tag{6}$$

where μ_0 and ϵ_0 denote the free-space permeability and permittivity, respectively, and the prime over the operator nabla indicates that the derivatives are with respect to the source coordinates. Furthermore, $\underline{\underline{\boldsymbol{G}}}^A$ and $\underline{\underline{\boldsymbol{G}}}^F$ are the DGF's for the magnetic and electric vector potentials, respectively, K^Φ and K^Ψ are the corresponding scalar potential kernels, and C^Φ and C^Ψ are the *correction factors* associated with the longitudinal electric and magnetic currents, respectively [60]. Note that $\nabla \cdot \boldsymbol{J}$ and $\nabla \cdot \boldsymbol{M}$ are proportional to, respectively, the electric and magnetic charge densities.

When the mixed-potential representations (5) and (6) are used in (1) and (2) to express the scattered fields radiated by $(\boldsymbol{J}_s, \boldsymbol{M}_s)$, one obtains the MPIE's. Apart from the dyadic nature of the vector potential kernels, these MPIE's are similar in form to their free-space counterparts and, thus, are amenable to the well-established numerical solution procedures developed for the latter [34], [35], [37], [89], [93].

III. Scalarization of Maxwell's Equations

Consider a uniaxially anisotropic, possibly lossy medium, which is transversely unbounded with respect to the z axis and is characterized, relative to free space, by z-dependent, in general complex-valued permeability and permittivity dyadics, $\underline{\underline{\mu}} = \underline{\underline{\boldsymbol{I}}}_t \mu_t + \hat{\boldsymbol{z}}\hat{\boldsymbol{z}}\mu_z$ and $\underline{\underline{\epsilon}} = \underline{\underline{\boldsymbol{I}}}_t \epsilon_t + \hat{\boldsymbol{z}}\hat{\boldsymbol{z}}\epsilon_z$, respectively, where $\underline{\underline{\boldsymbol{I}}}_t$ is the transverse unit dyadic. We wish to compute the fields $(\boldsymbol{E}, \boldsymbol{H})$ at an arbitrary point $\boldsymbol{r}$ due to a specified current distribution $(\boldsymbol{J}, \boldsymbol{M})$, as illustrated in Fig. 2(a). These fields are governed by the Maxwell's equations [77, p. 745]

$$\nabla \times \boldsymbol{E} = -j\omega\mu_0 \underline{\underline{\boldsymbol{\mu}}} \cdot \boldsymbol{H} - \boldsymbol{M}$$
$$\nabla \times \boldsymbol{H} = j\omega\epsilon_0 \underline{\underline{\boldsymbol{\epsilon}}} \cdot \boldsymbol{E} + \boldsymbol{J}. \tag{7}$$

Since the medium is homogeneous and of infinite extent in any transverse (to z) plane, the analysis is facilitated by the Fourier transformation of all fields with respect to the transverse coordinates. Hence, we express any scalar field component as $f(\boldsymbol{r}) \equiv f(\boldsymbol{\rho}; z)$, where $\boldsymbol{\rho} = \hat{\boldsymbol{x}}x + \hat{\boldsymbol{y}}y$ is the projection of $\boldsymbol{r}$ on the (x, y) plane, and introduce the Fourier transform pair

$$\mathcal{F} f(\boldsymbol{r}) \equiv \tilde{f}(\boldsymbol{k}_\rho; z) = \int_{-\infty}^{+\infty} \int_{-\infty}^{+\infty} f(\boldsymbol{r}) e^{j\boldsymbol{k}_\rho \cdot \boldsymbol{\rho}} \, dx \, dy \tag{8}$$

$$\mathcal{F}^{-1} \tilde{f}(\boldsymbol{k}_\rho; z) \equiv f(\boldsymbol{r}) = \frac{1}{(2\pi)^2} \int_{-\infty}^{+\infty} \int_{-\infty}^{+\infty} \tilde{f}(\boldsymbol{k}_\rho; z) e^{-j\boldsymbol{k}_\rho \cdot \boldsymbol{\rho}} \, dk_x \, dk_y \tag{9}$$

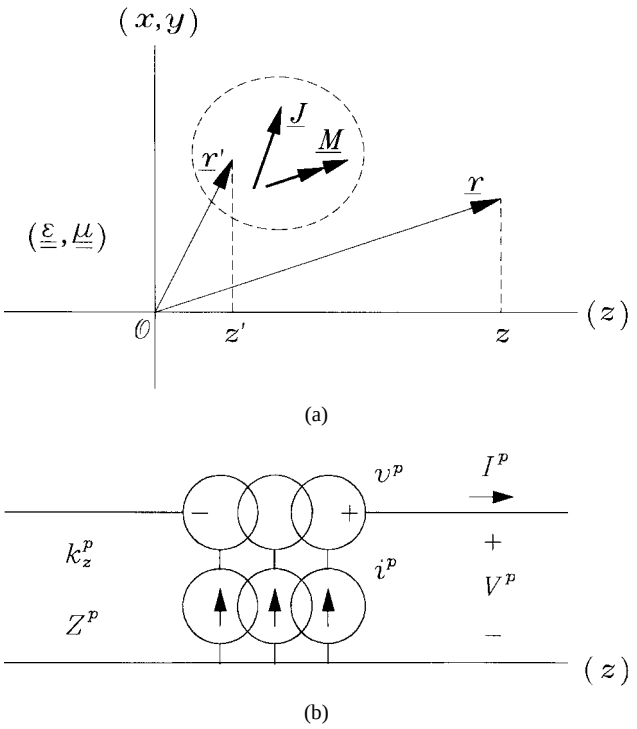

Fig. 2. Currents radiating in a uniaxial medium. (a) Physical configuration. (b) Transmission-line analog.

where $\boldsymbol{k}_\rho = \hat{\boldsymbol{x}}k_x + \hat{\boldsymbol{y}}k_y$. Upon applying (8) to (7), and separating the transverse and longitudinal parts of the resulting equations, one obtains

$$\frac{d}{dz}\tilde{\boldsymbol{E}}_t = \frac{1}{j\omega\epsilon_0\epsilon_t}(k_t^2 - \nu^e \boldsymbol{k}_\rho \boldsymbol{k}_\rho \cdot)(\tilde{\boldsymbol{H}}_t \times \hat{\boldsymbol{z}}) + \boldsymbol{k}_\rho \frac{\tilde{J}_z}{\omega\epsilon_0\epsilon_z} - \tilde{\boldsymbol{M}}_t \times \hat{\boldsymbol{z}} \tag{10}$$

$$\frac{d}{dz}\underline{\tilde{H}}_t = \frac{1}{j\omega\mu_0\mu_t}(k_t^2 - \nu^h \boldsymbol{k}_\rho \boldsymbol{k}_\rho \cdot)(\hat{z} \times \underline{\tilde{E}}_t) + \boldsymbol{k}_\rho \frac{\tilde{M}_z}{\omega\mu_0\mu_z} - \hat{z} \times \underline{\tilde{J}}_t \tag{11}$$

$$-j\omega\epsilon_0\epsilon_z\tilde{E}_z = j\boldsymbol{k}_\rho \cdot (\underline{\tilde{H}}_t \times \hat{\boldsymbol{z}}) + \tilde{J}_z \tag{12}$$

$$-j\omega\mu_0\mu_z\tilde{H}_z = j\boldsymbol{k}_\rho \cdot (\hat{z} \times \underline{\tilde{E}}_t) + \tilde{M}_z \tag{13}$$

where $k_t = k_0\sqrt{\mu_t\epsilon_t}$, $k_0 = \omega\sqrt{\mu_0\epsilon_0}$ being the free-space wavenumber, and where $\nu^e = \epsilon_t/\epsilon_z$ and $\nu^h = \mu_t/\mu_z$ are referred to as, respectively, the electric and magnetic anisotropy ratios. The subsequent analysis is greatly simplified if one defines a rotated spectrum-domain coordinate system based on $(\boldsymbol{k}_\rho, \hat{\boldsymbol{z}} \times \boldsymbol{k}_\rho)$ (see Fig. 3), with the unit vectors $(\hat{\boldsymbol{u}}, \hat{\boldsymbol{v}})$ given by [94]

$$\hat{\boldsymbol{u}} = \frac{k_x}{k_\rho}\hat{\boldsymbol{x}} + \frac{k_y}{k_\rho}\hat{\boldsymbol{y}}$$
$$\hat{\boldsymbol{v}} = -\frac{k_y}{k_\rho}\hat{\boldsymbol{x}} + \frac{k_x}{k_\rho}\hat{\boldsymbol{y}} \tag{14}$$

where $k_\rho = \sqrt{k_x^2 + k_y^2}$. If we now express the transverse electric and magnetic fields as

$$\tilde{\boldsymbol{E}}_t = \hat{\boldsymbol{u}}V^e + \hat{\boldsymbol{v}}V^h$$
$$\tilde{\boldsymbol{H}}_t \times \hat{\boldsymbol{z}} = \hat{\boldsymbol{u}}I^e + \hat{\boldsymbol{v}}I^h \tag{15}$$

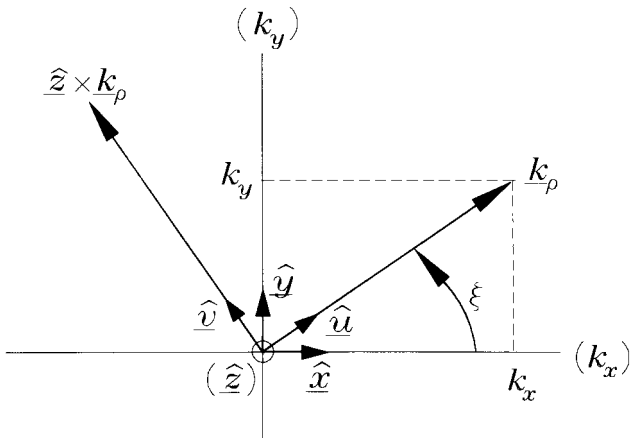

Fig. 3. Rotated spectrum-domain coordinate system.

and project (10) and (11) on $\hat{\boldsymbol{u}}$ and $\hat{\boldsymbol{v}}$, we find that these equations decouple into two sets of transmission line equations of the form

$$\frac{dV^p}{dz} = -jk_z^p Z^p I^p + v^p,$$
$$\frac{dI^p}{dz} = -jk_z^p Y^p V^p + i^p \tag{16}$$

where the superscript p assumes the values of e or h. Hence, the components of $\tilde{\boldsymbol{E}}_t$ and $\tilde{\boldsymbol{H}}_t$ in the (u, v) plane may be interpreted as voltages and currents on a transmission-line analog of the medium along the z axis, which was anticipated in the notation introduced in (15). The propagation wavenumbers and the characteristic impedances and admittances of this transmission line are given as

$$k_z^p = \sqrt{k_t^2 - \nu^p k_\rho^2} \tag{17}$$

$$Z^e = \frac{1}{Y^e} = \frac{k_z^e}{\omega\epsilon_0\epsilon_t}$$
$$Z^h = \frac{1}{Y^h} = \frac{\omega\mu_0\mu_t}{k_z^h} \tag{18}$$

where the square root branch in (17) is specified by the condition that $-\pi < \arg\{k_z^p\} \leq 0$. The voltage and current sources in (16) are given by

$$v^e = \frac{k_\rho}{\omega\epsilon_0\epsilon_z}\tilde{J}_z - \tilde{M}_v, \qquad i^e = -\tilde{J}_u$$
$$i^h = -\frac{k_\rho}{\omega\mu_0\mu_z}\tilde{M}_z - \tilde{J}_v, \qquad v^h = \tilde{M}_u. \tag{19}$$

In view of (15) and (12), (13), the spectral fields may now be expressed as

$$\tilde{\boldsymbol{E}} = \hat{\boldsymbol{u}}V^e + \hat{\boldsymbol{v}}V^h - \hat{\boldsymbol{z}}\frac{1}{j\omega\epsilon_0\epsilon_z}(jk_\rho I^e + \tilde{J}_z) \tag{20}$$

$$\tilde{\boldsymbol{H}} = -\hat{\boldsymbol{u}}I^h + \hat{\boldsymbol{v}}I^e + \hat{\boldsymbol{z}}\frac{1}{j\omega\mu_0\mu_z}(jk_\rho V^h - \tilde{M}_z) \tag{21}$$

which indicate that outside the source region (V^e, I^e) and (V^h, I^h) represent fields that are, respectively, TM and TE to z. The space-domain fields $(\boldsymbol{E}, \boldsymbol{H})$ are obtained from (20) and (21) via the inverse transform (9).

The original vector problem of Fig. 2(a) has thus been reduced to the scalar transmission line problem of Fig. 2(b). Note that—since the superscript p represents e or h—two

transmission lines are involved and associated, respectively, with the TM and TE partial fields.

IV. Dyadic Green's Functions

Consider the solutions of the transmission line equations (16) for unit-strength impulsive sources. Hence, let $V_i^p(z|z')$ and $I_i^p(z|z')$ denote the voltage and current, respectively, at z due to a 1-A shunt current source at z', and let $V_v^p(z|z')$ and $I_v^p(z|z')$ denote the voltage and current, respectively, at z due to a 1-V series voltage source at z' (see Fig. 4). Then, it follows from (16) that these TLGF's satisfy the following:

$$\begin{aligned}\frac{dV_i^p}{dz} &= -jk_z^pZ^pI_i^p\\ \frac{dI_i^p}{dz} &= -jk_z^pY^pV_i^p+\delta(z-z')\end{aligned} \tag{22}$$

$$\begin{aligned}\frac{dV_v^p}{dz} &= -jk_z^pZ^pI_v^p+\delta(z-z')\\ \frac{dI_v^p}{dz} &= -jk_z^pY^pV_v^p\end{aligned} \tag{23}$$

where δ is the Dirac delta, and that they possess the reciprocity properties [77, p. 194]

$$\begin{aligned}V_i^p(z|z') &= V_i^p(z'|z)\\ I_v^p(z|z') &= I_v^p(z'|z)\\ V_v^p(z|z') &= -I_i^p(z'|z)\\ I_i^p(z|z') &= -V_v^p(z'|z).\end{aligned} \tag{24}$$

The linearity of the transmission line equations (16) allows one to obtain (V^p, I^p) at any point z via the superposition integrals

$$\begin{aligned}V^p &= \langle V_i^p,\, i^p\rangle + \langle V_v^p,\, v^p\rangle\\ I^p &= \langle I_i^p,\, i^p\rangle + \langle I_v^p,\, v^p\rangle.\end{aligned} \tag{25}$$

Upon substituting these equations into (20) and (21) and using (19), one obtains spectrum-domain counterparts of (3) and (4), viz.

$$\tilde{\boldsymbol{E}} = \langle \tilde{\underline{\underline{\boldsymbol{G}}}}^{EJ};\, \tilde{\boldsymbol{J}}\rangle + \langle \tilde{\underline{\underline{\boldsymbol{G}}}}^{EM};\, \tilde{\boldsymbol{M}}\rangle \tag{26}$$

$$\tilde{\boldsymbol{H}} = \langle \tilde{\underline{\underline{\boldsymbol{G}}}}^{HJ};\, \tilde{\boldsymbol{J}}\rangle + \langle \tilde{\underline{\underline{\boldsymbol{G}}}}^{HM};\, \tilde{\boldsymbol{M}}\rangle \tag{27}$$

where the spectral DGF's $\tilde{\underline{\underline{\boldsymbol{G}}}}^{PQ}(\boldsymbol{k}_\rho;\, z|z')$ are given as

$$\begin{aligned}\tilde{\underline{\underline{\boldsymbol{G}}}}^{EJ} &= -\hat{\boldsymbol{u}}\hat{\boldsymbol{u}}V_i^e - \hat{\boldsymbol{v}}\hat{\boldsymbol{v}}V_i^h + \hat{\boldsymbol{z}}\hat{\boldsymbol{u}}\frac{k_\rho}{\omega\epsilon_0\epsilon_z}I_i^e + \hat{\boldsymbol{u}}\hat{\boldsymbol{z}}\frac{k_\rho}{\omega\epsilon_0\epsilon_z'}V_v^e\\ &\quad + \hat{\boldsymbol{z}}\hat{\boldsymbol{z}}\frac{1}{j\omega\epsilon_0\epsilon_z'}\left[\frac{k_\rho^2}{j\omega\epsilon_0\epsilon_z}I_v^e - \delta(z-z')\right]\end{aligned} \tag{28}$$

$$\tilde{\underline{\underline{\boldsymbol{G}}}}^{HJ} = \hat{\boldsymbol{u}}\hat{\boldsymbol{v}}I_i^h - \hat{\boldsymbol{v}}\hat{\boldsymbol{u}}I_i^e - \hat{\boldsymbol{z}}\hat{\boldsymbol{v}}\frac{k_\rho}{\omega\mu_0\mu_z}V_i^h + \hat{\boldsymbol{v}}\hat{\boldsymbol{z}}\frac{k_\rho}{\omega\epsilon_0\epsilon_z'}I_v^e \tag{29}$$

$$\begin{aligned}\tilde{\underline{\underline{\boldsymbol{G}}}}^{EM} &= -\hat{\boldsymbol{u}}\hat{\boldsymbol{v}}V_v^e + \hat{\boldsymbol{v}}\hat{\boldsymbol{u}}V_v^h + \hat{\boldsymbol{z}}\hat{\boldsymbol{v}}\frac{k_\rho}{\omega\epsilon_0\epsilon_z}I_v^e\\ &\quad - \hat{\boldsymbol{v}}\hat{\boldsymbol{z}}\frac{k_\rho}{\omega\mu_0\mu_z'}V_i^h\end{aligned} \tag{30}$$

$$\begin{aligned}\tilde{\underline{\underline{\boldsymbol{G}}}}^{HM} &= -\hat{\boldsymbol{u}}\hat{\boldsymbol{u}}I_v^h - \hat{\boldsymbol{v}}\hat{\boldsymbol{v}}I_v^e + \hat{\boldsymbol{z}}\hat{\boldsymbol{u}}\frac{k_\rho}{\omega\mu_0\mu_z}V_v^h + \hat{\boldsymbol{u}}\hat{\boldsymbol{z}}\frac{k_\rho}{\omega\mu_0\mu_z'}I_i^h\\ &\quad + \hat{\boldsymbol{z}}\hat{\boldsymbol{z}}\frac{1}{j\omega\mu_0\mu_z'}\left[\frac{k_\rho^2}{j\omega\mu_0\mu_z}V_i^h - \delta(z-z')\right].\end{aligned} \tag{31}$$

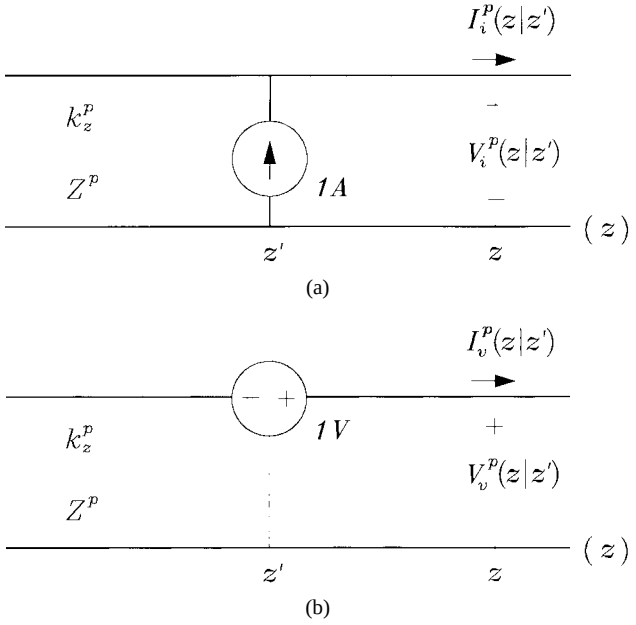

Fig. 4. Network problems for the determination of the transmission-line Green's functions.

In the above, the primed media parameters are evaluated at the source coordinate z', and this convention is used throughout this paper. The space-domain DGF's follow from (28)–(31) upon first projecting the unit vectors $(\hat{\boldsymbol{u}}, \hat{\boldsymbol{v}})$ on the (k_x, k_y)-coordinate system via (14) and then applying the inverse transformation (9). In view of the translational symmetry of the medium with respect to the transverse coordinates, we may write

$$\underline{\underline{\boldsymbol{G}}}^{PQ}(\boldsymbol{r}|\boldsymbol{r}') \equiv \underline{\underline{\boldsymbol{G}}}^{PQ}(\boldsymbol{\rho}-\boldsymbol{\rho}';\, z|z') \tag{32}$$

where

$$\underline{\underline{\boldsymbol{G}}}^{PQ}(\boldsymbol{\rho};\, z|z') = \mathcal{F}^{-1}\tilde{\underline{\underline{\boldsymbol{G}}}}^{PQ}(\boldsymbol{k}_\rho;\, z|z'). \tag{33}$$

The spectral integrals that arise in (33) may be expressed as

$$\mathcal{F}^{-1}\left\{\begin{matrix}\sin\\ \cos\end{matrix} n\xi\tilde{f}(k_\rho)\right\} = (-j)^n\begin{matrix}\sin\\ \cos\end{matrix} n\varphi\,\mathcal{S}_n\{\tilde{f}(k_\rho)\},\quad n=0,\,1,\,2 \tag{34}$$

where

$$\mathcal{S}_n\{\tilde{f}(k_\rho)\} = \frac{1}{2\pi}\int_0^\infty \tilde{f}(k_\rho)J_n(k_\rho\rho)k_\rho\,dk_\rho \tag{35}$$

is referred to as a Sommerfeld integral. Here, J_n is the Bessel function of order n and (ρ, φ) are the cylindrical coordinates of the projection of the field point on the (x, y) plane. Note that although (34) and (35) correspond to the case where the source is on the z axis, they are easily generalized for arbitrary source locations by the substitutions

$$\begin{aligned}\rho &\to \varrho = |\boldsymbol{\rho}-\boldsymbol{\rho}'|,\\ \varphi &\to \phi = \arctan\frac{y-y'}{x-x'}.\end{aligned} \tag{36}$$

The spectral DGF's (28)–(31) may directly be used in integral-equation formulations based on the spectral domain approach (SDA) [95]–[97]. The SDA and the space-domain integral equation technique are formally equivalent, and only

differ in the order in which the spatial and spectral integrations are performed. However, the SDA is less flexible in terms of the geometries it can handle and is in general less efficient than the space-domain MPIE, because it leads to double spectral integrals rather than Sommerfeld integrals [98].

V. Mixed Potential Representations

Consider first the case where only electric currents are present. It is then permissible to express the fields in terms of vector and scalar potentials through the equations

$$\begin{aligned} \mu_0 \underline{\underline{\boldsymbol{\mu}}} \cdot \boldsymbol{H} &= \nabla \times \boldsymbol{A} \\ \boldsymbol{E} &= -j\omega \boldsymbol{A} - \nabla \Phi. \end{aligned} \tag{37}$$

The linearity of the problem allows us to write

$$\boldsymbol{A} = \mu_0 \langle \underline{\underline{\boldsymbol{G}}}^A ; \boldsymbol{J} \rangle \tag{38}$$

where $\underline{\underline{\boldsymbol{G}}}^A(\boldsymbol{r}|\boldsymbol{r}')$ is the vector potential DGF. From (4) and (37) (with $\boldsymbol{M} = \boldsymbol{0}$) it follows that

$$\underline{\underline{\boldsymbol{\mu}}} \cdot \underline{\underline{\boldsymbol{G}}}^{HJ} = \nabla \times \underline{\underline{\boldsymbol{G}}}^A. \tag{39}$$

Since $\underline{\underline{\boldsymbol{G}}}^{HJ}$ has already been determined, we will use this relationship to obtain $\underline{\underline{\boldsymbol{G}}}^A$. The derivations are simplified in the spectrum domain, where the operator nabla becomes $\tilde{\nabla} = -jk_\rho \hat{\boldsymbol{u}} + \hat{\boldsymbol{z}} d/dz$. Clearly, (39) does not uniquely specify $\underline{\underline{\boldsymbol{G}}}^A$, making different formulations possible [60]. Here, we postulate the form

$$\underline{\underline{\tilde{\boldsymbol{G}}}}^A = \underline{\underline{\boldsymbol{I}}}_t \tilde{G}^A_{vv} + \hat{\boldsymbol{z}}\hat{\boldsymbol{u}} \tilde{G}^A_{zu} + \hat{\boldsymbol{z}}\hat{\boldsymbol{z}} \tilde{G}^A_{zz} \tag{40}$$

which is consistent with the Sommerfeld's choice of potentials [99, p. 258] for a horizontal Hertzian dipole over a dielectric half-space. This is more evident when (40) is projected on the Cartesian-coordinate system via (14) and put in the matrix form

$$[\tilde{G}^A] = \begin{bmatrix} \tilde{G}^A_{vv} & 0 & 0 \\ 0 & \tilde{G}^A_{vv} & 0 \\ \dfrac{k_x}{k_\rho} \tilde{G}^A_{zu} & \dfrac{k_y}{k_\rho} \tilde{G}^A_{zu} & \tilde{G}^A_{zz} \end{bmatrix} \tag{41}$$

which indicates that horizontal and vertical components of the vector potential are involved for a horizontal current source. To find the components of $\underline{\underline{\tilde{\boldsymbol{G}}}}^A(\boldsymbol{k}_\rho; z|z')$, we substitute (29) and (40) into the spectrum-domain counterpart of (39), which leads to the equations

$$j\omega\mu_0 \tilde{G}^A_{vv} = V_i^h \tag{42}$$

$$j\omega\mu_0 \tilde{G}^A_{zz} = \eta_0^2 \frac{\mu_t}{\epsilon'_z} I_v^e \tag{43}$$

$$\frac{d}{dz} \tilde{G}^A_{vv} + jk_\rho \tilde{G}^A_{zu} = -\mu_t I_i^e \tag{44}$$

where $\eta_0 = \sqrt{\mu_0/\epsilon_0}$ is the intrinsic impedance of free space. From (42) and (44), upon using (18) and (22), we finally obtain

$$j\omega\mu_0 \tilde{G}^A_{zu} = \frac{\omega\mu_0\mu_t}{k_\rho} (I_i^h - I_i^e). \tag{45}$$

The scalar potential may be found from the auxiliary condition

$$\nabla \cdot (\mu_t^{-1} \mu_z^{-1} \underline{\underline{\boldsymbol{\mu}}} \cdot \boldsymbol{A}) = -j\omega\mu_0\epsilon_0\epsilon_t \Phi \tag{46}$$

which can be shown to be consistent with the vector potential obtained above. To arrive at the mixed-potential form of $\boldsymbol{E}$, we postulate the decomposition

$$\epsilon_t^{-1} \nabla \cdot (\mu_t^{-1} \mu_z^{-1} \underline{\underline{\boldsymbol{\mu}}} \cdot \underline{\underline{\boldsymbol{G}}}^A) = -\nabla' K^\Phi + C^\Phi \hat{\boldsymbol{z}} \tag{47}$$

where K^Φ is the scalar potential kernel and C^Φ is the *correction factor*, which arises in general when both horizontal and vertical current components are present [41], [42], [60]. To find K^Φ and C^Φ, we substitute (40) in the spectrum-domain counterpart of (47) and, noting that $\tilde{\nabla}' = jk_\rho \hat{\boldsymbol{u}} + \hat{\boldsymbol{z}} d/dz'$, we obtain

$$\tilde{K}^\Phi = \frac{1}{j\omega\mu_0\mu_z\epsilon_t} V_i^h + \frac{1}{k_\rho^2 \epsilon_t} \frac{d}{dz} (I_i^h - I_i^e) \tag{48}$$

$$\tilde{C}^\Phi = \frac{1}{j\omega\epsilon_0\epsilon'_z\epsilon_t} \frac{d}{dz} I_v^e + \frac{d}{dz'} \tilde{K}^\Phi \tag{49}$$

which upon using (22) and (23) yield

$$-\frac{\tilde{K}^\Phi}{j\omega\epsilon_0} = \frac{1}{k_\rho^2} (V_i^h - V_i^e) \tag{50}$$

$$-\frac{\tilde{C}^\Phi}{j\omega\epsilon_0} = \frac{j\omega\mu_0\mu'_t}{k_\rho^2} (V_v^h - V_v^e). \tag{51}$$

The space-domain counterparts of the spectral kernels derived above can be expressed in terms of the Sommerfeld integrals via (34)–(36). Hence, we find

$$\begin{aligned} G^A_{xx}(\boldsymbol{\rho}; z|z') &= G^A_{yy}(\boldsymbol{\rho}; z|z') \\ &= \mathcal{S}_0\{\tilde{G}^A_{vv}(k_\rho; z|z')\} \end{aligned} \tag{52}$$

$$G^A_{zz}(\boldsymbol{\rho}; z|z') = \mathcal{S}_0\{\tilde{G}^A_{zz}(k_\rho; z|z')\} \tag{53}$$

$$G^A_{zx}(\boldsymbol{\rho}; z|z') = -j \cos\varphi \, \mathcal{S}_1\{\tilde{G}^A_{zu}(k_\rho; z|z')\} \tag{54}$$

$$G^A_{zy}(\boldsymbol{\rho}; z|z') = -j \sin\varphi \, \mathcal{S}_1\{\tilde{G}^A_{zu}(k_\rho; z|z')\} \tag{55}$$

$$K^\Phi(\boldsymbol{\rho}; z|z') = \mathcal{S}_0\{\tilde{K}^\Phi(k_\rho; z|z')\} \tag{56}$$

$$C^\Phi(\boldsymbol{\rho}; z|z') = \mathcal{S}_0\{\tilde{C}^\Phi(k_\rho; z|z')\}. \tag{57}$$

We next substitute (46) and (47) in the second equation of (37) and, after some transformations involving the Gauss' theorem, arrive at

$$\boldsymbol{E} = -j\omega\mu_0 \langle \underline{\underline{\boldsymbol{G}}}^A ; \boldsymbol{J} \rangle + \frac{1}{j\omega\epsilon_0} \nabla (\langle K^\Phi, \nabla' \cdot \boldsymbol{J} \rangle + \langle C^\Phi \hat{\boldsymbol{z}}; \boldsymbol{J} \rangle) \tag{58}$$

which is the desired mixed-potential representation of $\boldsymbol{E}$. Note that the kernels in the above are given as Sommerfeld integrals of spectral functions, for which explicit expressions in terms of the TLGF's have been derived.

When only magnetic currents are present, the analysis is dual to that given above. The mixed-potential representation for $\boldsymbol{H}$ may be obtained from the above formulas by the following replacements of symbols: $\boldsymbol{E} \to \boldsymbol{H}$, $\boldsymbol{J} \to \boldsymbol{M}$, $\boldsymbol{A} \to \boldsymbol{F}$, $\Phi \to \Psi$, $\epsilon \to \mu$, $\mu \to \epsilon$, $V \to I$, $I \to V$, $v \to i$, $i \to v$, $e \to h$, and $h \to e$. In the general case, where both electric and magnetic currents are present, we use superposition and, in view of (3) and (4), arrive at the mixed-potential forms (5) and (6).

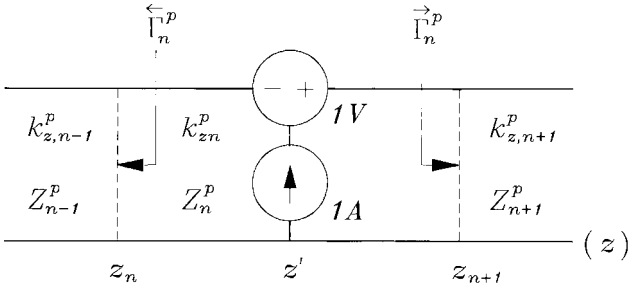

Fig. 5. Voltage and current point sources in a transmission-line section.

Finally, we point out that the correction term in (58) may be grouped with the vector potential term, resulting in an alternative mixed-potential representation, which corresponds to formulation C of Michalski and Zheng [60]. For planar conductors, this formulation reduces to that of Mosig and Gardiol [38].

VI. Transmission-Line Green's Functions

The formulation developed so far is for an unspecified stratification, since no assumption has been made regarding the z dependence of the media parameters. We now specialize it to the case of a multilayered medium with piecewise-constant parameters. The parameters pertaining to layer n with boundaries at z_n and z_{n+1} are distinguished by a subscript n. The transmission line analog of the layered medium consists of a cascade connection of uniform transmission line sections, where section n with terminals at z_n and z_{n+1} has propagation constant k_{zn}^p and characteristic impedance Z_n^p. To find the TLGF's, we excite the transmission line network by unit-strength voltage and current sources at z' in section n and compute the voltage and current at z in section m. Hence, the primed media parameters assume the values pertaining to layer n, while the unprimed ones are those of layer m. The source section is illustrated in Fig. 5, where $\overleftarrow{\Gamma}_n^p$ and $\overrightarrow{\Gamma}_n^p$ are the voltage reflection coefficients looking to the left and right, respectively, out of the terminals of section n. These coefficients, which are referred to z_n and z_{n+1}, respectively, may be computed from the relations

$$\overleftarrow{\Gamma}_{n+1}^p = \frac{\Gamma_{n,n+1}^p + \overleftarrow{\Gamma}_n^p t_n^p}{1 + \Gamma_{n,n+1}^p \overleftarrow{\Gamma}_n^p t_n^p} \tag{59}$$

$$\overrightarrow{\Gamma}_{n-1}^p = \frac{\Gamma_{n,n-1}^p + \overrightarrow{\Gamma}_n^p t_n^p}{1 + \Gamma_{n,n-1}^p \overrightarrow{\Gamma}_n^p t_n^p} \tag{60}$$

where

$$\Gamma_{ij}^p = \frac{Z_i^p - Z_j^p}{Z_i^p + Z_j^p} \tag{61}$$

and $t_n^p = e^{-j2k_{zn}^p d_n}$ with $d_n = z_{n+1} - z_n$. These formulas follow from the source-free transmission line equations (16) and the continuity of the voltages and currents at the line junctions. One applies (59) and (60) recursively beginning at, respectively, the left and the right ends of the transmission line network.

Consider first the case $m = n$, when z is within the source section. The TLGF V_i^p is then readily determined from (22) as

$$V_i^p(z|z') = \frac{Z_n^p}{2}\left[e^{-jk_{zn}^p|z-z'|} + \frac{1}{D_n^p}\sum_{s=1}^{4} R_{ns}^p e^{-jk_{zn}^p \gamma_{ns}}\right] \tag{62}$$

where

$$D_n^p = 1 - \overleftarrow{\Gamma}_n^p \overrightarrow{\Gamma}_n^p t_n^p \tag{63}$$

$$\begin{aligned} R_{n1}^p &= \overrightarrow{\Gamma}_n^p \\ R_{n2}^p &= \overleftarrow{\Gamma}_n^p \\ R_{n3}^p &= R_{n4}^p = \overleftarrow{\Gamma}_n^p \overrightarrow{\Gamma}_n^p \end{aligned} \tag{64}$$

$$\begin{aligned} \gamma_{n1} &= 2z_{n+1} - (z + z') \\ \gamma_{n2} &= (z + z') - 2z_n \\ \gamma_{n3} &= 2d_n + (z - z') \\ \gamma_{n4} &= 2d_n - (z - z'). \end{aligned} \tag{65}$$

The first term in (62) represents the direct ray between the source and the field point, while the second term represents the rays that undergo partial reflections at the upper and lower slab boundaries before reaching the observation point. The remaining TLGF's may readily be derived from (62) upon using (22)–(24). For example, one may obtain I_i^p from V_i^p via the first equation of (22), from which V_v^p follows via the third equation of (24). The result is

$$V_v^p(z|z') = \frac{1}{2}\left[\pm e^{-jk_{zn}^p|z-z'|} - \frac{1}{D_n^p}\sum_{s=1}^{4}(-1)^s R_{ns}^p e^{-jk_{zn}^p \gamma_{ns}}\right] \tag{66}$$

where the upper and lower signs pertain to $z > z'$ and $z < z'$, respectively. To conserve space, we do not list the expressions for I_v^p and I_i^p which, as is evident from (22) and (23), are dual to those for V_i^p and V_v^p, respectively, and may be obtained from the latter by replacing the impedances by admittances (which has also the effect of changing the signs of the reflection coefficients). Observe that the discontinuous terms appearing in V_v^p and I_i^p cancel out when the TE and TM TLGF's are subtracted to form $\tilde{G}^{\Phi}$ and $\tilde{G}_{zu}^{A}$.

Consider next the case $m < n$, when z is outside the source section and $z < z'$. Given the voltage $V^p(z_n)$ across the left terminals of section n, the voltage $V^p(z)$ and current $I^p(z)$ at any point z in section m can be found from the homogeneous form of the transmission-line equations (16) as [100]

$$\begin{Bmatrix} V^p(z) \\ I^p(z) \end{Bmatrix} = V^p(z_n) \frac{\prod_{k=m+1}^{n-1} \overleftarrow{T}_k^p}{1 + \overleftarrow{\Gamma}_m^p t_m^p} \times \begin{Bmatrix} \overleftarrow{\tau}_m^p(z) \\ \overleftarrow{y}_m^p(z) \end{Bmatrix} e^{-jk_{zm}^p(z_{m+1} - z)} \tag{67}$$

where

$$\overleftarrow{T}_k^p \equiv \frac{V^p(z_k)}{V^p(z_{k+1})} = \frac{(1 + \overleftarrow{\Gamma}_k^p)\theta_k^p}{1 + \overleftarrow{\Gamma}_k^p t_k^p} \tag{68}$$

with $\theta_k^p = e^{-jk_{kz}^p d_k}$, and where

$$\overleftarrow{\tau}_m^p(z) = [1 + \overleftarrow{\Gamma}_m^p e^{-j2k_{zm}^p(z - z_m)}] \tag{69}$$

$$\overleftarrow{y}_m^p(z) = -Y_m^p[1 - \overleftarrow{\Gamma}_m^p e^{-j2k_{zm}^p(z - z_m)}]. \tag{70}$$

It is understood that the product in (67) is equal to one if the lower limit exceeds the upper limit. Note that (67) is applicable irrespective of the source type. Hence, if section n is excited by a unit-strength current source at z', then $V^p(z_n) = V_i^p(z_n|z')$, and $V^p(z)$ and $I^p(z)$ represent $V_i^p(z|z')$ and $I_i^p(z|z')$, respectively. If, on the other hand, section n is excited by a unit-strength voltage source at z', then $V^p(z_n) = V_v^p(z_n|z')$, and $V^p(z)$ and $I^p(z)$ represent $V_v^p(z|z')$ and $I_v^p(z|z')$, respectively.

Analogous formulas may be developed for the case $m > n$, when z is outside the source section and $z > z'$. However, this is hardly necessary because the reciprocity theorems (24) allow one to interchange the source and field point locations. For example, $V_v^p(z|z')$ may be computed as $-I_i^p(z'|z)$. This application of reciprocity also results in a shorter and more efficient computer code.

VII. Discussion of Sommerfeld Integrals

The computation of the Sommerfeld integrals (35) is a difficult task because of the in general oscillatory and divergent behavior of the integrands and the occurrence of singularities near the integration path in the complex k_ρ plane [44], [45]. Since these integrals must be repeatedly evaluated in filling of the MOM matrix, their efficient computation is of paramount importance and has been the subject of much research. Nevertheless, it is fair to say that a completely satisfactory solution to this problem is still lacking, especially in the case of arbitrarily shaped objects extending over more than one layer of the multilayered medium. A detailed treatment of the Sommerfeld integration being outside the scope of this article, here we only highlight some of the techniques involved.

The integrand singularities, which occur in complex-conjugate pairs in the second and fourth quadrants of the k_ρ plane, consist of poles and branch points [101, p. 111]. In the lossless case some of these singularities appear on the real axis and the integration path in (35) must be indented into the first quadrant to avoid them. The branch points only occur for vertically unbounded media, i.e., when the top and/or the bottom layer is a half-space. In this case, the integration path must approach infinity on the proper sheet of the Riemann surface associated with the longitudinal propagation wavenumbers (17) of the half-spaces. The poles are associated with the TM and TE guided waves and are found as roots of the resonant denominator (63) in any finite-thickness layer, or as roots of the denominator of the reflection coefficient (59) or (60) looking into the layered medium from a half-space. The number of poles is in general infinite, but only a finite number of them appear on the proper sheet in the case of vertically unbounded media. Various integration paths in the k_ρ plane have been employed [38], [61], [102], [103], but the real-axis path, indented into the first quadrant to avoid the branch-point and pole singularities [104], has proven to be most convenient for multilayered media, because it obviates the need to locate the poles. When $\varrho > 0$, the integral over the real axis tail of the path may be computed as a sum of an alternating series of integrals between zeros of the Bessel function. To speed up the convergence, series acceleration techniques, such as the method of averages [38], [45], [105] or the continued fraction expansion [106], may then be applied.

Even with the state-of-the-art techniques, the Sommerfeld integrals may take a significant part of the overall computational effort involved in the solution of the MPIE. One attractive remedy is to precompute these integrals on a grid of points in the solution domain and to use table look-up and interpolation techniques. For arbitrarily shaped objects, 3-D interpolation in ϱ, z, and z' is required [2], except for objects confined to a single layer, when one may split the kernels into parts depending on $(\varrho, z - z')$ and $(\varrho, z + z')$, and compute them separately using 2-D interpolations [102]. Only 1-D interpolation in ϱ is needed for strictly planar microstrip structures, which leads to a particularly efficient solution procedure [45], [105].

Another approach, which came into prominence recently, is the discrete complex image method (DCIM) [52], [107]–[113]. The basic idea of the DCIM is to extract from the spectral kernel its quasistatic part and its guided wave terms, and to approximate the remainder function by a sum of complex exponentials, using an established systems identification procedure [114]. The Sommerfeld integrals are then evaluated in closed form via the Sommerfeld identity [101, p. 66]. Since DCIM obviates numerical integration, it affords at least an order-of-magnitude speed-up in the MOM matrix fill time [115]. However, to gain this advantage, the objects must be confined to a single layer and the quasi-static terms must be invertible in closed form. Also, DCIM has no built-in convergence measures and its accuracy can only be ascertained *a posteriori* by checking the results against those obtained by Sommerfeld integration. Furthermore, the application of this method in multilayered media is currently impeded by the lack of reliable automated procedures for the extraction of the guided wave poles.

VIII. Shielded Environments

Although the formulation presented so far can easily accommodate horizontal perfectly conducting or impedance ground planes, the underlying assumption has been that the layered medium is of infinite lateral extent. We now extend this theory to the practically important case of a layered medium enclosed by a rectangular shield with PEC walls. The cross-sectional dimensions of the shield are $a \times b$, as illustrated in Fig. 6. Note that the shield forms a rectangular waveguide along the z axis [116], or a rectangular cavity—if it is sandwiched between horizontal ground planes [117]. Here, we represent the effect of the side walls by a set of image sources radiating in a laterally unbounded medium [81, p. 103], [118], which makes it possible to take advantage of the formulation developed in the preceding sections. We then convert the image representations to the formally equivalent modal (spectrum-domain) expansions.

To begin with, consider a point charge q located at (x', y', z') inside the rectangular shield and its three images located at $(-x', y', z')$, $(x', -y', z')$, and $(-x', -y', z')$, as illustrated in Fig. 6. Note that the polarities (signs) of these images are consistent with the boundary conditions at two

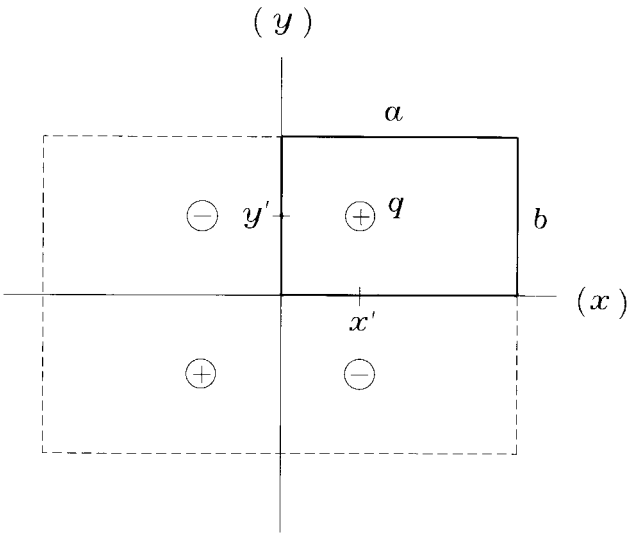

Fig. 6. Point charge inside a rectangular shield and its images in the $x = 0$ and $y = 0$ PEC planes.

TABLE I
IMAGE SIGN COEFFICIENTS FOR ELECTRIC SOURCES

Source	s_x	s_y
J_x	$+1$	-1
J_y	-1	$+1$
q, J_z	-1	-1

intersecting PEC ground planes defined by $x = 0$ and $y = 0$. The so-constructed four-source set (the original source plus the three images) forms the *basic image set* (BIS). Note that the BIS is located within the $2a \times 2b$ *reference cell* centered at $(x, y) = (0, 0)$. Similar image sets may be constructed for x-, y-, and z-oriented current elements. The polarities of the images for different sources are conveniently described by two sign coefficients, s_x and s_y, where $s_\nu = +1$ if the polarity of the image in the $\nu = 0$ PEC wall is the same as that of the original source, and $s_\nu = -1$ if the imaged source undergoes a sign reversal. The values of s_x and s_y for electric sources are listed in Table I. For magnetic sources, all signs should be reversed.

To maintain the correct boundary conditions at the four side walls, the BIS of the reference cell must be imaged in the $x = a$ and $y = b$ PEC planes, and the new image sets must again be imaged in the $x = 0$ and $y = 0$ planes, etc. As a result, a doubly periodic lattice of BIS's is obtained, with periods $2a$ and $2b$ along the x and y axes, respectively. Since these sources are now embedded in a transversely unbounded medium, they may be analyzed within the framework of the theory developed in the previous sections. Hence, if $G(x - x', z - z'; z|z')$ is a scalar potential kernel or a scalar component of a dyadic kernel (or Green's function) in the *laterally open medium*, we find that the corresponding kernel, $\mathcal{G}$, in the *laterally shielded environment* is given by

$$\begin{aligned}\mathcal{G}(\boldsymbol{r}|\boldsymbol{r}') = \sum_{m=-\infty}^{+\infty}\sum_{n=-\infty}^{+\infty} & \times \{G(x - x' + 2ma,\, y - y' + 2nb;\, z|z') \\ & + s_x G(x + x' - 2ma, y - y' + 2nb;\, z|z') \\ & + s_y G(x - x' + 2ma,\, y + y' - 2nb;\, z|z') \\ & + s_x s_y G(x + x' - 2ma,\, y + y' - 2nb;\, z|z')\}. \end{aligned} \tag{71}$$

The sign coefficients s_x and s_y in the above depend on the type of the kernel or Green's function considered. For example, if G represents G^A_{zx}, which is the z component of the vector potential Green's function due to an x-directed current element, we find from Table I that $s_x = +1$ and $s_y = -1$. For the scalar potential and correction kernels K^Φ and C^Φ, the sign coefficients are those associated with q.

The spatial sum (71) may be transformed by the Poisson's formula [119, p. 47] into the spectral sum [120]

$$\begin{aligned}\mathcal{G}(\mathbf{r}|\mathbf{r}') = \frac{1}{4ab}\sum_{m=-\infty}^{+\infty}\sum_{n=-\infty}^{+\infty} & \times \tilde{G}(k_{xm}, k_{yn}; z|z') e^{-j(k_{xm}x + k_{yn}y)} \\ & \times (e^{jk_{xm}x'} + s_x e^{-jk_{xm}x'})(e^{jk_{yn}y'} + s_y e^{-jk_{yn}y'}) \end{aligned} \tag{72}$$

where $k_{xm} = m\pi/a$, $k_{yn} = n\pi/b$. Furthermore, the series in the above may be folded, with the result

$$\begin{aligned}\mathcal{G}(\mathbf{r}|\mathbf{r}') = \frac{1}{ab}\sum_{m=0}^{\infty}\sum_{n=0}^{\infty} & \varepsilon_m \varepsilon_n \tilde{G}(k_{xm}, k_{yn}; z|z') \\ & \times T_x(k_{xm}x) S_x(k_{xm}x') T_y(k_{yn}y) S_y(k_{yn}y') \end{aligned} \tag{73}$$

where $\varepsilon_n = 1$ for $n = 0$ and $\varepsilon_n = 2$ for $n > 0$, and where

$$S_\nu(\xi) = \begin{cases} \cos\xi, & s_\nu = +1 \\ j\sin\xi & s_\nu = -1 \end{cases} \tag{74}$$

$$T_\nu(\xi) = \begin{cases} \cos\xi & s_\nu \cdot c_\nu = +1 \\ -j\sin\xi & s_\nu \cdot c_\nu = -1 \end{cases}. \tag{75}$$

We have introduced in the above the sign coefficients c_x and c_y, defined as follows: $c_\nu = +1$ (-1) if $\tilde{G}$ is an even (odd) function of k_ν. For example, if G represents G^A_{zx}, the inspection of (41) and (45) indicates that $c_x = -1$ and $c_y = +1$. When the reference cell in Fig. 6 is centered at an arbitrary point (x_0, y_0), rather than at $(0, 0)$, the above formulas must be modified by the substitutions $(x, y) \to (x - x_0, y - y_0)$ and $(x', y') \to (x' - x_0, y' - y_0)$.

The double series in (73) is slowly convergent, especially when $z = z'$, which is often the case in the analysis of planar microstrip structures, and must in practice be accelerated. This may be accomplished by subtracting from $\tilde{G}$ its quasistatic form, $\tilde{G}^\infty$, which converts (73) into a rapidly converging series, because $\tilde{G}$ and $\tilde{G}^\infty$ have the same asymptotic behavior. The double series of the subtracted quasistatic terms is then added back in its spatial form (71). Since the latter is comprised of the direct and quasistatic

image terms, it is amenable to the well-established acceleration methods [70], [121]–[124]. These techniques employ mixed-domain representations involving both a space-domain and a spectrum-domain series and have an arbitrary parameter which distributes the computational burden between the two domains. In a simpler approach [125], [126], one of the asymptotic series is left in the space domain and the other is transformed via a 1-D Poisson's formula, leading to a rapidly convergent series of modified Bessel functions of the second kind. The quasi-static terms must be invertible in closed form for these techniques to be applicable.

IX. Conclusion

We have presented a simple derivation of the dyadic Green's functions for plane-stratified, multilayered, uniaxial media, based on the transmission-line network analog along the axis normal to the stratification [77]. Within the framework of this transmission-line formalism, we have also derived mixed-potential integral equations (MPIE's) for arbitrarily shaped, conducting or penetrable objects embedded in the multilayered medium. The formulation presented here is compact and computationally efficient, and it affords much insight into the various Green's functions and kernels, because the behavior of the transmission-line voltages and currents—which are governed by the simple telegraphist's equations—is well understood. The MPIE's derived here are well-suited for the analysis of inhomogeneities buried in layered earth and for the modeling of integrated dielectric waveguides, probe-fed and aperture-coupled microstrip patch antennas and arrays, as well as complex microwave integrated circuits—including those comprising vertical transitions, air-bridges, and vias. There has been a definite trend recently to use MPIE's even for strictly planar microstrip structures. Among the integral equation formulations, the space-domain MPIE approach is, in our experience, the most versatile and efficient way to analyze complex 3-D objects embedded in multilayered media.

Acknowledgment

The authors would like to thank D. R. Wilton, University of Houston, TX, for many personal communications regarding the subject of this paper.

References

[1] A. Karlsson and G. Kristensson, "Electromagnetic scattering from subterranean obstacles in a stratified ground," *Radio Sci.*, vol. 18, pp. 345–356, May/June 1983.
[2] P. E. Wannamaker, G. W. Hohmann, and W. A. SanFilipo, "Electromagnetic modeling of three-dimensional bodies in layered earths using integral equations," *Geophys.*, vol. 49, pp. 60–74, Jan. 1984.
[3] R. H. Hardman and L. C. Shen, "Theory of induction sonde in dipping beds," *Geophys.*, vol. 51, pp. 800–809, Mar. 1986.
[4] L. Tsang, E. Njoku, and J. A. Kong, "Microwave thermal emission from a stratified medium with nonuniform temperature distribution," *J. Appl. Phys.*, vol. 46, pp. 5127–5133, Dec. 1975.
[5] J. R. Wait, *Wave Propagation Theory*. New York: Pergamon, 1981.
[6] G. P. S. Cavalcante, D. A. Rogers, and A. J. Giarola, "Analysis of electromagnetic wave propagation in multilayered media using dyadic Green's functions," *Radio Sci.*, vol. 17, pp. 503–508, May/June 1982.
[7] W. P. Harokopus and P. B. Katehi, "Radiation losses in microstrip antenna feed networks printed on multilayer substrates," *Int. J. Numer. Mod.*, vol. 4, pp. 3–18, 1991.
[8] N. Faché, F. Olyslager, and D. De Zutter, *Electromagnetic and Circuit Modeling of Multiconductor Transmission Lines*. Oxford: Clarendon, 1993.
[9] A. K. Bhattacharyya, *Electromagnetic Fields in Multilayered Structures*. Boston, MA: Artech House, 1994.
[10] E. Arbel and L. B. Felsen, "Theory of radiation from sources in anisotropic media, Part 1: General sources in stratified media," in *Electromagnetic Theory and Antennas, Part 1*, E. C. Jordan, Ed. New York: Macmillan, 1963, pp. 391–420.
[11] V. G. Daniele and R. S. Zich, "Radiation by arbitrary sources in anisotropic stratified media," *Radio Sci.*, vol. 8, pp. 63–70, Jan. 1973.
[12] S. M. Ali and S. F. Mahmoud, "Electromagnetic fields of buried sources in stratified anisotropic media," *IEEE Trans. Antennas Propagat.*, vol. AP-27, pp. 671–678, Sept. 1979.
[13] J. K. Lee and J. A. Kong, "Dyadic Green's functions for layered anisotropic medium," *Electromagn.*, vol. 3, pp. 111–130, 1983.
[14] T. Sphicopoulos, V. Teodoridis, and F. E. Gardiol, "Dyadic Green function for the electromagnetic field in multilayered isotropic media: An operator approach," *Inst. Elect. Eng. Proc.*, vol. 132, pt. H, pp. 329–334, Aug. 1985.
[15] J. S. Bagby, D. P. Nyquist, and B. C. Drachman, "Integral formulation for analysis of integrated dielectric waveguides," *IEEE Trans. Microwave Theory Tech.*, vol. MTT-33, pp. 906–915, Oct. 1985.
[16] D. H. S. Cheng, "On the formulation of the dyadic Green's function in a layered medium," *Electromagn.*, vol. 6, no. 2, pp. 171–182, 1986.
[17] C. M. Krowne, "Determination of the Green's function in the spectral domain using a matrix method: Application to radiators immersed in a complex anisotropic layered medium," *IEEE Trans. Antennas Propagat.*, vol. AP-34, pp. 247–253, Feb. 1986.
[18] N. K. Das and D. M. Pozar, "A generalized spectral-domain Green's function for multilayer dielectric substrates with application to multilayer transmission lines," *IEEE Trans. Microwave Theory Tech.*, vol. MTT-35, pp. 326–335, Mar. 1987.
[19] L. Beyne and D. De Zutter, "Green's function for layered lossy media with special application to microstrip antennas," *IEEE Trans. Microwave Theory Tech.*, vol. 36, pp. 875–881, May 1988.
[20] L. Vegni, R. Cicchetti, and P. Capece, "Spectral dyadic Green's function formulation for planar integrated structures," *IEEE Trans. Antennas Propagat.*, vol. 36, pp. 1057–1065, Aug. 1988.
[21] R. Kastner, E. Heyman, and A. Sabban, "Spectral domain iterative analysis of single- and double-layered microstrip antennas using the conjugate gradient algorithm," *IEEE Trans. Antennas Propagat.*, vol. 36, pp. 1204–1212, Sept. 1988.
[22] E. W. Kolk, N. H. G. Baken, and H. Blok, "Domain integral equation analysis of integrated optical channel and ridge waveguides in stratified media," *IEEE Trans. Microwave Theory Tech.*, vol. 38, pp. 78–85, Jan. 1990.
[23] J. F. Kiang, S. M. Ali, and J. A. Kong, "Integral equation solution to the guidance and leakage properties of coupled dielectric strip waveguides," *IEEE Trans. Microwave Theory Tech.*, vol. 38, pp. 193–203, Feb. 1990.
[24] T. M. Habashy, S. M. Ali, J. A. Kong, and M. D. Grossi, "Dyadic Green's functions in a planar, stratified, arbitrarily magnetized linear plasma," *Radio Sci.*, vol. 26, pp. 701–715, May/June 1991.
[25] S. M. Ali, T. M. Habashy, and J. A. Kong, "Spectral-domain dyadic Green's function in layered chiral media," *J. Opt. Soc. Amer. A*, vol. 9, pp. 413–423, Mar. 1992.
[26] S. Barkeshli and P. H. Pathak, "On the dyadic Green's function for a planar multilayered dielectric/magnetic media," *IEEE Trans. Microwave Theory Tech.*, vol. 40, pp. 128–142, Jan. 1992.
[27] H. J. M. Bastiaansen, N. H. G. Baken, and H. Blok, "Domain-integral analysis of channel waveguides in anisotropic multi-layered media," *IEEE Trans. Microwave Theory Tech.*, vol. 40, pp. 1918–1926, Oct. 1992.
[28] S. Barkeshli, "On the electromagnetic dyadic Green's functions for planar multi-layered anisotropic uniaxial material media," *Int. J. Infrared Millimeter Waves*, vol. 13, no. 4, pp. 507–527, 1992.
[29] P. Bernardi and R. Cicchetti, "Dyadic Green's functions for conductor-backed layered structures excited by arbitrary tridimensional sources," *IEEE Trans. Microwave Theory Tech.*, vol. 42, pp. 1474–1483, Aug. 1994.
[30] S.-G. Pan and I. Wolff, "Scalarization of dyadic spectral Green's functions and network formalism for three-dimensional full-wave analysis of planar lines and antennas," *IEEE Trans. Microwave Theory Tech.*, vol. 42, pp. 2118–2127, Nov. 1994.
[31] A. Dreher, "A new approach to dyadic Green's function in spectral domain," *IEEE Trans. Antennas Propagat.*, vol. 43, pp. 1297–1302, Nov. 1995.
[32] R. F. Harrington, *Field Computation by Moment Methods*. New York:

Macmillan, 1968; Melbourne, FL: Krieger, reprint 1982.
[33] J. C. Chao, Y. J. Liu, F. J. Rizzo, P. A. Martin, and L. Udpa, "Regularized integral equations for curvilinear boundary elements for electromagnetic wave scattering in three dimensions," *IEEE Trans. Antennas Propagat.*, vol. 43, pp. 1416–1422, Dec. 1995.
[34] A. W. Glisson and D. R. Wilton, "Simple and efficient numerical methods for problems of electromagnetic radiation and scattering from surfaces," *IEEE Trans. Antennas Propagat.*, vol. AP-28, pp. 593–603, Sept. 1980.
[35] S. M. Rao, D. R. Wilton, and A. W. Glisson, "Electromagnetic scattering by surfaces of arbitrary shape," *IEEE Trans. Antennas Propagat.*, vol. AP-30, pp. 409–418, May 1982.
[36] D. H. Schaubert, D. R. Wilton, and A. W. Glisson, "A tetrahedral modeling method for electromagnetic scattering by arbitrarily shaped inhomogeneous dielectric bodies," *IEEE Trans. Antennas Propagat.*, vol. AP-32, pp. 77–85, Jan. 1984.
[37] K. Umashankar, A. Taflove, and S. M. Rao, "Electromagnetic scattering by arbitrary shaped three-dimensional homogeneous lossy dielectric objects," *IEEE Trans. Antennas Propagat.*, vol. AP-34, pp. 758–766, June 1986.
[38] J. R. Mosig and F. E. Gardiol, "A dynamical radiation model for microstrip structures," in *Advances in Electronics and Electron Physics*, P. W. Hawkes, Ed. New York: Academic, 1982, vol. 59, pp. 139–237.
[39] ———, "Analytic and numerical techniques in the Green's function treatment of microstrip antennas and scatterers," *Inst. Elect. Eng. Proc.*, vol. 130, pt. H, pp. 175–182, Mar. 1983.
[40] ———, "General integral equation formulation for microstrip antennas and scatterers," *Inst. Elect. Eng. Proc.*, vol. 132, pt. H, pp. 424–432, Dec. 1985.
[41] K. A. Michalski, "The mixed-potential electric field integral equation for objects in layered media," *Arch. Elek. Übertragung.*, vol. 39, pp. 317–322, Sept./Oct. 1985.
[42] ———, "On the scalar potential of a point charge associated with a time-harmonic dipole in a layered medium," *IEEE Trans. Antennas Propagat.*, vol. AP-35, pp. 1299–1301, Nov. 1987.
[43] R. C. Hall and J. R. Mosig, "The analysis of coaxially fed microstrip antennas with electrically thick substrates," *Electromagn.*, vol. 9, no. 4, pp. 367–384, 1989.
[44] J. R. Mosig, "Integral equation technique," in *Numerical Techniques for Microwave and Millimeter—Wave Passive Structures*, T. Itoh, Ed. New York: Wiley, 1989, pp. 133–213.
[45] J. R. Mosig, R. C. Hall, and F. E. Gardiol, "Numerical analysis of microstrip patch antennas," in *Handbook of Microstrip Antennas*, J. R. James and P. S. Hall, Eds. London: Peregrinus, 1989, pp. 391–453.
[46] H. Legay, R. Gillard, J. Citerne, and G. Piton, "Via-hole effects on radiation characteristics of a patch microstrip antenna coaxially fed through the ground plane," *Ann. Télécommun.*, vol. 46, no. 7/8, pp. 367–381, 1991.
[47] D. Zheng and K. A. Michalski, "Analysis of arbitrarily shaped coax-fed microstrip antennas—A hybrid mixed-potential integral equation approach," *Microwave Opt. Tech. Lett.*, vol. 3, pp. 200–203, June 1990.
[48] G. A. E. Vandenbosch and A. R. Van de Capelle, "Mixed-potential integral expression formulation of the electric field in a stratified dielectric medium—Application to the case of a probe current source," *IEEE Trans. Antennas Propagat.*, vol. 40, pp. 806–817, July 1992.
[49] P. Pichon, J. R. Mosig, and A. Papiernik, "Input impedance of arbitrarily shaped microstrip antennas," *Electron. Lett.*, vol. 24, pp. 1214–1215, Sept. 1988.
[50] W. Wertgen and R. H. Jansen, "Efficient direct and iterative electrodynamic analysis of geometrically complex MIC and MMIC structures," *Int. J. Numer. Mod.*, vol. 2, pp. 153–186, 1989.
[51] L. Barlatey, J. R. Mosig, and T. Sphicopoulos, "Analysis of stacked microstrip patches with a mixed potential integral equation," *IEEE Trans. Antennas Propagat.*, vol. 38, pp. 608–615, May 1990.
[52] K.-L. Wu, J. Litva, R. Fralich, and C. Wu, "Full-wave analysis of arbitrarily shaped line-fed microstrip antennas using triangular finite-element method," *Inst. Elect. Eng. Proc.*, vol. 138, pt. H, pp. 421–428, Oct. 1991.
[53] A. Hoorfar, J. X. Zheng, and D. C. Chang, "Numerical modeling of crossover and other junction discontinuities in two-layer microstrip circuits," *Int. J. Microwave Millimeter-Wave Comput.-Aided Eng.*, vol. 2, no. 4, pp. 261–272, 1992.
[54] F. Alonso-Monferrer, A. A. Kishk, and A. W. Glisson, "Green's function analysis of planar circuits in a two-layer grounded medium," *IEEE Trans. Antennas Propagat.*, vol. 40, pp. 690–696, June 1992.
[55] L. Barlatey, H. Smith, and J. Mosig, "Printed radiating structures and transitions in multilayered substrates," *Int. J. Microwave Millimeter-Wave Comput.-Aided Eng.*, vol. 2, no. 4, pp. 273–285, 1992.
[56] T. K. Sarkar, P. Midya, Z. A. Maricevic, M. Kahrizi, S. M. Rao, and A. R. Djordjevic, "Analysis of arbitrarily shaped microstrip patch antennas using the Sommerfeld formulation," *Int. J. Microwave Millimeter-Wave Comput.-Aided Eng.*, vol. 2, no. 3, pp. 168–178, 1992.
[57] R. D. Cloux, G. P. J. F. M. Maas, and A. J. H. Wachters, "Quasistatic boundary element method for electromagnetic simulation of PCBS," *Philips J. Res.*, vol. 48, no. 1/2, pp. 117–144, 1994.
[58] J. Sercu, N. Faché, F. Libbrecht, and P. Lagasse, "Mixed potential integral equation technique for hybrid microstrip-slotline multilayered circuits using a mixed rectangular-triangular mesh," *IEEE Trans. Microwave Theory Tech.*, vol. 43, pp. 1162–1172, May 1995.
[59] L. Giauffret and J.-M. Laheurte, "Theoretical and experimental characterization of CPW-fed microstrip antennas," *Inst. Elect. Eng Proc. Microwave Antennas Propagat.*, vol. 143, pp. 13–17, Feb. 1996.
[60] K. A. Michalski and D. Zheng, "Electromagnetic scattering and radiation by surfaces of arbitrary shape in layered media, Part I: Theory," *IEEE Trans. Antennas Propagat.*, vol. 38, pp. 335–344, Mar. 1990.
[61] ———, "Electromagnetic scattering and radiation by surfaces of arbitrary shape in layered media, Part II: Implementation and results for contiguous half-spaces," *IEEE Trans. Antennas Propagat.*, vol. 38, pp. 345–352, Mar. 1990.
[62] W. A. Johnson, "Analysis of vertical, tubular cylinder which penetrates an air-dielectric interface and which is excited by an azimuthally symmetric source," *Radio Sci.*, vol. 18, pp. 1273–1281, Nov./Dec. 1983.
[63] K. A. Michalski, C. E. Smith, and C. M. Butler, "Analysis of a horizontal two-element array antenna above a dielectric halfspace," *Inst. Elect. Eng. Proc.*, vol. 132, pt. H, pp. 335–338, Aug. 1985.
[64] S. Singh and D. R. Wilton, "Analysis of an infinite periodic array of slot radiators with dielectric loading," *IEEE Trans. Antennas Propagat.*, vol. 39, pp. 190–196, Feb. 1991.
[65] K. A. Michalski and D. Zheng, "Rigorous analysis of open microstrip lines of arbitrary cross section in bound and leaky regimes," *IEEE Trans. Microwave Theory Tech.*, vol. 37, pp. 2005–2010, Dec. 1989.
[66] D. Zheng and K. A. Michalski, "Analysis of coaxially fed microstrip antennas of arbitrary shape with thick substrates," *J. Electromagn. Waves Applicat.*, vol. 5, no. 12, pp. 1303–1327, 1991.
[67] K. A. Michalski and D. Zheng, "Analysis of microstrip resonators of arbitrary shape," *IEEE Trans. Antennas Propagat.*, vol. 40, pp. 112–119, Jan. 1992.
[68] N. J. Champagne, J. T. Williams, and D. R. Wilton, "Analysis of resistively loaded, printed spiral antennas," *Electromagn.*, vol. 14, pp. 363–395, July/Dec. 1994.
[69] N. W. Montgomery and D. R. Wilton, "Analysis of arbitrary conducting periodic structures embedded in layered media," in *Dig. IEEE AP-S Int. Symp.*, London, ON, Canada, June 1991, pp. 1889–1892.
[70] D. R. Wilton, "Review of current status and trends in the use of integral equations in computational electromagnetics," *Electromagn.*, vol. 12, pp. 287–341, July/Dec. 1992.
[71] J. Chen, A. A. Kishk, and A. W. Glisson, "MPIE for conducting sheets penetrating a multilayer medium," in *Dig. IEEE AP-S Int. Symp.*, Seattle, WA, June 1994, pp. 1346–1349.
[72] K. A. Michalski, "Mixed-potential integral equation (MPIE) formulation for nonplanar microstrip structures of arbitrary shape in multilayered uniaxial media," *Int. J. Microwave Millimeter-Wave Comput.-Aided Eng.*, vol. 3, no. 4, pp. 420–431, 1993.
[73] ———, "Formulation of mixed-potential integral equations for arbitrarily shaped microstrip structures with uniaxial substrates," *J. Electromagn. Waves Applicat.*, vol. 7, no. 7, pp. 899–917, 1993.
[74] S. Vitebskiy and L. Carin, "Moment method modeling of short-pulse scattering from and the resonances of a wire buried inside a lossy, dispersive half-space," *IEEE Trans. Antennas Propagat.*, vol. 43, pp. 1303–1312, Nov. 1995.
[75] A. Abdelmageed, K. A. Michalski, and A. W. Glisson, "Analysis of EM scattering by conducting bodies of revolution in layered media using the discrete complex image method," in *Dig. IEEE AP-S Int. Symp.*, Newport Beach, CA, June 1995, pp. 402–406.
[76] S. Vitebskiy, K. Sturgess, and L. Carin, "Short-pulse plane-wave scattering from buried perfectly conducting bodies of revolution," *IEEE Trans. Antennas Propagat.*, vol. 44, pp. 143–151, Feb. 1996.
[77] L. B. Felsen and N. Marcuvitz, *Radiation and Scattering of Waves.* Englewood Cliffs, NJ: Prentice Hall, 1973.
[78] N. G. Alexopoulos, "Integrated-circuit structures on anisotropic substrates," *IEEE Trans. Microwave Theory Tech.*, vol. MTT-33, pp. 847–881, Oct. 1985.
[79] D. M. Pozar, "Radiation and scattering from a microstrip patch on a uniaxial substrate," *IEEE Trans. Antennas Propagat.*, vol. AP-35, pp. 613–621, June 1987.
[80] Z. Xiong, Y. Luo, S. Wang, and G. Wu, "Induced-polarization and

electromagnetic modeling of a three-dimensional body buried in a two-layer anisotropic earth," *Geophys.*, vol. 51, pp. 2235–2246, Dec. 1986.
[81] R. F. Harrington, *Time-Harmonic Electromagnetic Field.* New York: McGraw-Hill, 1961.
[82] ——, "Boundary integral formulations for homogeneous material bodies," *J. Electromagn. Waves Applicat.*, vol. 3, no. 1, pp. 1–15, 1989.
[83] K. H. Lee, D. F. Pridmore, and H. F. Morrison, "A hybrid three-dimensional electromagnetic modeling scheme," *Geophys.*, vol. 46, pp. 796–805, May 1981.
[84] J. Wu and K. A. Michalski, "Hybrid finite element—mixed-potential integral equation—discrete complex image approach for inhomogeneous waveguides in layered media," in *Dig. IEEE AP-S Int. Symp.*, Newport Beach, CA, June 1995, pp. 1472–1475.
[85] T. F. Eibert and V. Hansen, "FEM/BEM-hybrid approach for layered media," in *Dig. IEEE AP-S Int. Symp.*, Newport Beach, CA, June 1995, pp. 1464–1467.
[86] ——, "3-D FEM/BEM-hybrid approach for planar layered media," *Electromagn.*, to be published.
[87] X.-B. Xu and W. Yan, "Modification of hybrid integral equations for determining scattering by an inhomogeneous cylinder of discontinuous electromagnetic parameters near a media interface," *J. Electromagn. Waves Applicat.*, vol. 7, no. 10, pp. 1389–1394, 1993.
[88] A. A. Sebak and L. Shafai, "Performance of various integral equation formulations for numerical solution of scattering by impedance objects," *Can. J. Phys.*, vol. 62, pp. 605–615, 1984.
[89] A. W. Glisson, "Electromagnetic scattering by arbitrarily shaped surfaces with impedance boundary conditions," *Radio Sci.*, vol. 27, pp. 935–943, Nov./Dec. 1992.
[90] I. P. Theron and J. H. Cloete, "On the surface impedance used to model the conductor losses of microstrip structures," *Inst. Elect. Eng. Proc. Microwave Antennas Propagat.*, vol. 142, pp. 35–40, Feb. 1995.
[91] R. F. Harrington, "The method of moments in electromagnetics," *J. Electromagn. Waves Applicat.*, vol. 1, no. 3, pp. 181–200, 1987.
[92] C. M. Butler, Y. Rahmat-Samii, and R. Mittra, "Electromagnetic penetration through apertures in conducting surfaces," *IEEE Trans. Antennas Propagat.*, vol. AP-26, pp. 82–93, Jan. 1978.
[93] W. A. Johnson, D. R. Wilton, and R. M. Sharpe, "Modeling scattering from and radiation by arbitrarily shaped objects with the electric field integral equation triangular surface patch code," *Electromagn.*, vol. 10, no. 1/2, pp. 41–63, 1990.
[94] T. Itoh, "Spectral-domain immittance approach for dispersion characteristics of generalized printed transmission lines," *IEEE Trans. Microwave Theory Tech.*, vol. MTT-28, pp. 733–736, July 1980.
[95] W. C. Chew and Q. Liu, "Resonance frequency of a rectangular microstrip patch," *IEEE Trans. Antennas Propagat.*, vol. 36, pp. 1045–1056, Aug. 1988.
[96] T.-S. Horng, N. G. Alexopoulos, S.-C. Wu, and H.-Y. Yang, "Full-wave spectral analysis for open microstrip discontinuities of arbitrary shape including radiation and surface-wave losses," *Int. J. Microwave Millimeter-Wave Comput.-Aided Eng.*, vol. 2, no. 4, pp. 224–240, 1992.
[97] T. Becks and I. Wolff, "Analysis of 3-D metallization structures by a full-wave spectral domain technique," *IEEE Trans. Microwave Theory Tech.*, vol. 40, pp. 2219–2227, Dec. 1992.
[98] K. A. Michalski and D. Zheng, "Analysis of planar microstrip structures of arbitrary shape—To be, or not to be in the spectral domain?," in *Proc. Symp. Antennas Tech. Applicat. Electromagn.*, Winnipeg, Canada, Aug. 1990, pp. 240–245.
[99] A. Sommerfeld, *Partial Differential Equations in Physics.* New York: Academic, 1949.
[100] C.-I. G. Hsu, R. F. Harrington, K. A. Michalski, and D. Zheng, "Analysis of a multiconductor transmission lines of arbitrary cross-section in multilayered uniaxial media," *IEEE Trans. Microwave Theory Tech.*, vol. 41, pp. 70–78, Jan. 1993.
[101] W. C. Chew, *Waves and Fields in Inhomogeneous Media.* New York: Van Nostrand Reinhold, 1990.
[102] G. J. Burke, E. K. Miller, J. N. Brittingham, D. L. Lager, R. J. Lytle, and J. T. Okada, "Computer modeling of antennas near the ground," *Electromagn.*, vol. 1, pp. 29–49, Jan./Mar. 1981.
[103] K. A. Michalski, "On the efficient evaluation of integrals arising in the Sommerfeld halfspace problem," in *Moment Methods in Antennas and Scatterers*, R. C. Hansen, Ed. Boston, MA: Artech House, 1990, pp. 325–331.
[104] E. H. Newman and D. Forrai, "Scattering from a microstrip patch," *IEEE Trans. Antennas Propagat.*, vol. AP-35, pp. 245–251, Mar. 1987.
[105] L. T. Hildebrand and D. A. McNamara, "A guide to implementation aspects of the spatial-domain integral equation analysis of microstrip antennas," *Appl. Comput. Electromagn. Soc. J.*, vol. 10, no. 1, pp. 40–51, 1995.
[106] A. D. Chave, "Numerical integration of related Hankel transforms by quadrature and continued fraction expansion," *Geophys.*, vol. 48, pp. 1671–1686, Dec. 1983.
[107] D. G. Fang, J. J. Yang, and G. Y. Delisle, "Discrete image theory for horizontal electric dipoles in a multilayered medium," *Inst. Elect. Eng. Proc.*, vol. 135, pt. H, pp. 297–303, Oct. 1988.
[108] Y. L. Chow, J. J. Yang, D. G. Fang, and G. E. Howard, "A closed-form spatial Green's function for the thick microstrip substrate," *IEEE Trans. Microwave Theory Tech.*, vol. 39, pp. 588–592, Mar. 1991.
[109] M. I. Aksun and R. Mittra, "Derivation of closed-form Green's functions for a general microstrip geometry," *IEEE Trans. Microwave Theory Tech.*, vol. 40, pp. 2055–2062, Nov. 1992.
[110] R. A. Kipp and C. H. Chan, "Complex image method for sources in bounded regions of multilayer structures," *IEEE Trans. Microwave Theory Tech.*, vol. 42, pp. 860–865, May 1994.
[111] G. Dural and M. I. Aksun, "Closed-form Green's functions for general sources in stratified media," *IEEE Trans. Microwave Theory Tech.*, vol. 43, pp. 1545–1552, July 1995.
[112] M. I. Aksun, "A robust approach for the derivation of closed-form Green's functions," *IEEE Trans. Microwave Theory Tech.*, vol. 44, pp. 651–658, May 1996.
[113] K. A. Michalski and J. R. Mosig, "Discrete complex image mixed-potential integral equation analysis of coax-fed coupled vertical monopoles in a grounded dielectric substrate: Two formulations," *Inst. Elect. Eng. Proc. Microwave Antennas Propagat.*, vol. 142, pp. 269–274, June 1995.
[114] T. K. Sarkar and O. Pereira, "Using the matrix pencil method to estimate the parameters of a sum of complex exponentials," *IEEE Antennas Propagat. Mag.*, vol. 37, pp. 48–55, Feb. 1995.
[115] K. A. Michalski and J. R. Mosig, "Discrete complex image mixed-potential integral equation analysis of microstrip patch antennas with vertical probe feeds," *Electromagn.*, vol. 15, pp. 377–392, July/Aug. 1995.
[116] L.-W. Li, P.-S. Kooi, M.-S. Leong, T.-S. Yeo, and S.-L. Ho, "Input impedance of probe-excited semi-infinite rectangular waveguide with arbitrary multilayered loads: Part I—Dyadic Green's functions," *IEEE Trans. Microwave Theory Tech.*, vol. 43, pp. 1559–1566, July 1995.
[117] A. Hill, J. Burke, and K. Kottapalli, "Three-dimensional electromagnetic analysis of shielded microstrip circuits," *Int. J. Microwave Millimeter-Wave Comput.-Aided Eng.*, vol. 2, no. 4, pp. 286–296, 1992.
[118] R. W. Jackson, "The use of side images to compute package effects in MoM analysis of MMIC circuits," *IEEE Trans. Microwave Theory Tech.*, vol. 41, pp. 406–414, Mar. 1993.
[119] A. Papoulis, *The Fourier Integral and Its Applications.* New York: McGraw-Hill, 1962.
[120] M.-H. Ho, K. A. Michalski, and K. Chang, "Waveguide excited microstrip patch antenna—Theory and experiment," *IEEE Trans. Antennas Propagat.*, vol. 42, pp. 1114–1125, Aug. 1994.
[121] K. E. Jordan, G. R. Richter, and P. Sheng, "An efficient numerical evaluation of the Green's function for the Helmholtz operator on periodic structures," *J. Comp. Phys.*, vol. 63, pp. 222–235, 1986.
[122] E. Cohen, "Critical distance for grating lobe series," *IEEE Trans. Antennas Propagat.*, vol. 39, pp. 677–679, May 1991.
[123] S. Singh, W. F. Richards, J. R. Zinecker, and D. R. Wilton, "Accelerating the convergence of series representing the free space periodic Green's function," *IEEE Trans. Antennas Propagat.*, vol. 38, pp. 1958–1962, Dec. 1990.
[124] R. M. Shubair and Y. L. Chow, "Efficient computation of the periodic Green's function in layered media," *IEEE Trans. Microwave Theory Tech.*, vol. 41, pp. 498–502, Mar. 1993.
[125] J. Xu, "Fast convergent dyadic Green's function in a rectangular waveguide," *Int. J. Infrared Millimeter Waves*, vol. 14, no. 9, pp. 1789–1800, 1993.
[126] G. V. Eleftheriades, J. R. Mosig, and M. Gugliemi, "A fast integral equation technique for shielded planar circuits defined on nonuniform meshes," *IEEE Trans. Microwave Theory Tech.*, to be published.

Krzysztof A. Michalski (S'78–M'81–SM'88), for photography and biography, see p. 1125 of the August 1994 issue of this TRANSACTIONS.

Juan R. Mosig (S'76–M'79–M'87–SM'94), for photography and biography, see p. 197 of February 1995 issue of this TRANSACTIONS.